Joint Frame Synchronization and Carrier Frequency Offset Estimation in Multicarrier Systems

Zhongshan Zhang
University of Alberta
Edmonton, AB T6G 2V4, Canada
zszhang@ece.ualberta.ca

Hidetoshi Kayama
DoCoMo Beijing Labs Co., Ltd
Beijing, P.R.China
kayama@docomolabs-beijing.com.cn

C. Tellambura
University of Alberta
Edmonton, AB T6G 2V4, Canada
chintha@ece.ualberta.ca

***Abstract*— A novel joint frame synchronization and carrier frequency offset estimation scheme for burst transmission mode multi-carrier systems is proposed, which uses a Central-Symmetric and Comb-Like training sequence (CSCL). This time-domain Comb-Like shape eases its power detection at the receiver without increasing the total training sequence power. Fine frame synchronization as well as carrier frequency offset acquisition with a maximum acquisition range of $\pm\frac{N}{4\times SF}$ times the subcarrier spacing can also be performed based on the proposed training sequence, where N denotes the *Discrete Fourier Transform* (DFT) length and SF stands for an integer-valued *Spreading Factor* that is used to generate the proposed training sequence. The remaining carrier frequency offset after acquisition can be further estimated and corrected by using a Fine Adjustment algorithm. In order to reduce the performance loss introduces by a higher *Peak-to-Average Power Ratio* (PAPR) in the CSCL, a time-domain Constant-Envelop training sequence (CE) is also proposed in this paper, which outperforms CSCL-based algorithm. The comparison of the proposed algorithms with the SS (Shi&Serpedin) algorithm by computer simulation illustrates the superior performance of the proposed algorithm with regard to estimation accuracy.**

I. Introduction

Orthogonal frequency division multiplexing (OFDM) is an effective technique to combat multipath fading [1], [2]. In OFDM, the insertion of a guard interval between symbol blocks called cyclic prefix (CP) mitigates *Inter-Symbol Interference* (ISI). OFDM has been adopted as the modulation scheme for a DAB (*Digital Audio Broadcasting*) system [3], ADSL (Asymmetry Digital Subscriber Loop) [4] and is also adopted by the IEEE802.11a standard at the 5-GHz band with data rate up to 54Mb/s [5]. OFDM can also be combined with CDMA (code-division multiple-access), such as multicarrier-CDMA (MC-CDMA) and multicarrier DS-CDMA [6]. In a broadband channel with an approximate 50 to 100MHz bandwidth, *Variable Spreading Factor-Orthogonal Frequency and Code Division Multiplexing* (VSF-OFCDM) has been proposed by NTT DoCoMo, which is based on MC-CDMA and yet outperforms the conventional DS-CDMA in the forward link [7].

A high-speed and high performance synchronization scheme should be provided in burst transmission mode multicarrier modulation systems in order to detect and demodulate the transmitted signal correctly. Many frame synchronization algorithms are available in [8], [9], [10], [11], [12], [13], [14], [15], [16]. The algorithm given in [9] performs synchronization based on the cyclic-prefix in an OFDM symbol, which can only be applied to symbol synchronization. Null symbols can also be utilized to find the beginning of a frame [17]; however, null-based techniques fail when applied to burst transmission mode. Some estimators, either training symbol aided [11], [12] or not [9], [10], utilize the correlation between two parts of a received training sequence to perform synchronization. However, the timing metric of this kind of algorithm appears a large value at a position neighbored the training sequence start (the correct synchronization position), which degrades their synchronization performance.

Multicarrier systems are also sensitive to carrier frequency offset. Many existing algorithms for carrier frequency offset estimation transmit periodic patterns from the transmitter. Based on the phase rotations between these patterns at the receiver, carrier frequency offset can be estimated [11], [12], [19], [20], [21], [22], [15], [23]. The estimator proposed in [9] utilizes the cyclic prefix to estimate the carrier frequency offset, but the estimation range is limited within ± 0.5 subcarrier spacing. By exploiting the utilization of virtual subcarriers, high performance carrier frequency offset estimators can also be designed [17], [24]. Some algorithms are proposed for increasing the acquisition range [12], [19]. An improved carrier frequency offset estimator is also proposed in [18], which outperforms that proposed in [12].

In this paper, a new joint frame synchronization and carrier frequency offset estimation scheme for multicarrier system is proposed, which is based on a Central-Symmetric and Comb-Like (CSCL) training sequence. The boundary of the training sequence/frame can be found with high reliability based on the proposed training sequence. The maximum carrier frequency offset acquisition range in the proposed scheme is up to $\frac{N}{4\times SF}$ times the subcarrier spacing. A Maximum-Likelihood (ML) carrier frequency offset fine adjustment algorithm is also proposed based on CSCL to estimate and correct the residual carrier frequency offset after acquisition. In order to reduce the performance loss in the CSCL sequence due to PAPR, a time-domain Constant-Envelop training sequence (CE) is also proposed.

The remainder of this paper is organized as follows. Section II briefly introduces the system fundamentals. Section III proposes a new power detection and coarse frame synchronization

1-4244-0357-X/06/$20.00 ©2006 Crown Copyright
This full text paper was peer reviewed at the direction of IEEE Communications Society subject matter experts for publication in the IEEE GLOBECOM 2006 proceedings.

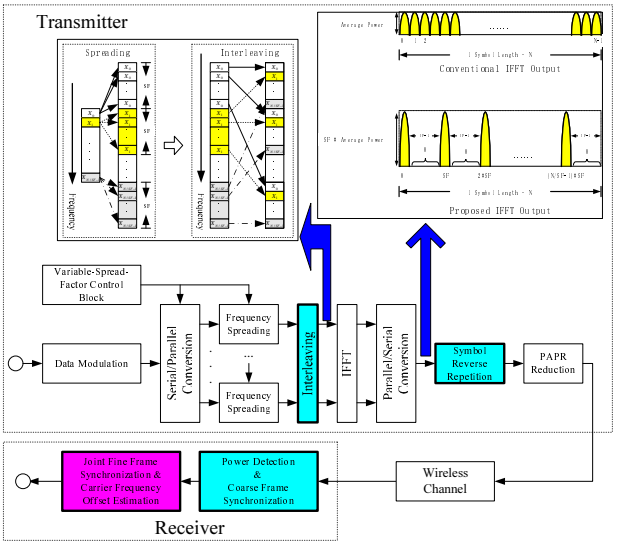

Fig. 1. Joint frame synchronization and carrier frequency offset estimation in burst transmission mode multicarrier systems.

algorithm based on the proposed Comb-like training symbol and analyzes its performance. A new CSCL-based joint fine frame synchronization and carrier frequency offset acquisition algorithm is given by Section IV, and a ML carrier frequency offset fine adjustment algorithm based on the same training sequence is proposed in Section V. A time-domain Constant-Envelop training sequence (CE) is proposed in Section VI for the purpose of PAPR reduction. Section VII provides the simulation results. Finally, Section VIII concludes the paper.

II. System Fundamentals

In conventional OFDM systems, the input symbols are complex numbers from a signal constellation (e.g., PSK, QAM). Let X_k denote the complex symbol modulated onto the k-th subcarrier. The output signal samples, $y(n)$, can be related to the input symbols by an *Inverse Discrete Fourier Transform* (IDFT), as given by

$$\begin{aligned} y(n) &= \frac{1}{N}\sum_{k=0}^{N-1} X_k \cdot e^{\frac{j2\pi nk}{N}} + w(n) \\ &= v(n) + w(n), \quad n = 0, 1, \cdots, N-1 \end{aligned} \tag{1}$$

where $v(n)$ denotes the IDFT output (signal part) and $w(n)$ denotes an *additive white Gaussian noise* (AWGN) term. The average *Signal-to-Noise Ratio* (SNR) in $y(n)$ is

$$\bar{\gamma} = \frac{\mathbb{E}\left\{\left|\frac{1}{N}\sum_{k=0}^{N-1} X_k \cdot e^{\frac{j2\pi nk}{N}}\right|^2\right\}}{\mathbb{E}\left\{|w(n)|^2\right\}} = \frac{\sigma_s^2}{\sigma_w^2}. \tag{2}$$

The proposed scheme is performed based on a Central-Symmetric and Comb-Like (CSCL) training sequence, which is composed of two training symbols with the second training symbol being the reverse replica of the first one. The first training symbol can be generated by modulating a frequency-domain training symbol $\mathbf{x} = \{\underbrace{X_0, X_1, \cdots, X_{N/SF-1}}_{subblock_1} \cdots \underbrace{X_0, X_1, \cdots, X_{N/SF-1}}_{subblock_{SF}}\}$, where SF is a pre-determined *Spreading Factor*, as illustrated in Fig.1. The IDFT output of $\mathbf{x}$ is a time-domain Comb-Like training symbol, as given by

$$\begin{aligned} v(n) &= \frac{1}{N}\sum_{k=0}^{N-1} X_k e^{\frac{j2\pi nk}{N}} \\ &= \frac{\sin(n\pi)}{N \cdot \sin(\frac{n\pi}{SF})} \cdot e^{\frac{j\pi n(SF-1)}{SF}} \sum_{k=0}^{N/SF-1} X_k \cdot e^{\frac{j2\pi nk}{N}} \end{aligned} \tag{3}$$

for $n = 0, 1, \cdots, N-1$. When $\frac{N}{SF}$ is large enough, from the Central Limit Theorem (CLT) we know that $v(n)$ can be approximated as a stationary Gaussian process of zero mean, and its variance $\sigma_v^2 = \mathbb{E}\left\{|v(n)|^2\right\}$ satisfies $\lim_{n=m\times SF} \mathbb{E}\left\{|v(n)|^2\right\} = SF \cdot \sigma_s^2$ and $\lim_{n\neq m\times SF} \mathbb{E}\left\{|v(n)|^2\right\} = 0$ where $m = 0, 1, \cdots, N/SF - 1$.

III. Power Detection and Coarse Frame Synchronization

In order to perform power detection at the receiver, we should first specify a *False Alarm* probability-P_{FA}, which is defined as the probability that noise is falsely seen as signal. By comparing the total power of $L(1 \le L \le N/SF)$ continuously received samples, i.e., $\Omega(n, L) = \sum_{m=0}^{L-1} |y(n + m \times SF)|^2$, with a decision threshold $L \times \Gamma$ (Γ being a pre-specified threshold), a new coming training sequence can be detected. It is reasonable to formulate $\Omega(n, L)$ as a central chi-square random variable with $2L$ degrees of freedom [25]. The probability that $\Omega(n, L)$ is smaller than $L \times \Gamma$ (*Miss Detection* probability) can be derived as

$$P_{MD}^L = 1 - (P_{FA})^{\frac{L}{SF\cdot\bar{\gamma}+1}} \cdot \sum_{i=0}^{L-1} \frac{1}{i!}\left(\frac{L \cdot ln(\frac{1}{P_{FA}})}{SF \cdot \bar{\gamma} + 1}\right)^i. \tag{4}$$

As compared to it, the *Miss Detection* probability in conventional OFDM systems (equivalent to the proposed scheme with $SF = 1$) is found to be

$$P_{Con}^L = 1 - (P_{FA})^{\frac{L}{\bar{\gamma}+1}} \cdot \sum_{i=0}^{L-1} \frac{1}{i!}\left(\frac{L \cdot ln\left(\frac{1}{P_{FA}}\right)}{\bar{\gamma} + 1}\right)^i \tag{5}$$

where $1 \le L < N$.

The proposed time-domain Comb-Like training symbol can improve the power detection performance, especially in a burst transmission mode system. Some conventional algorithms, e.g., [12], perform frame detection by exploiting the correlation in the training sequence. Frame detection as well as fine frame synchronization will be performed once a local peak of the timing metric is found, and the performance of this algorithm was analyzed in [12]. Fig.2 compares the frame

1-4244-0357-X/06/$20.00 ©2006 Crown Copyright
This full text paper was peer reviewed at the direction of IEEE Communications Society subject matter experts for publication in the IEEE GLOBECOM 2006 proceedings.

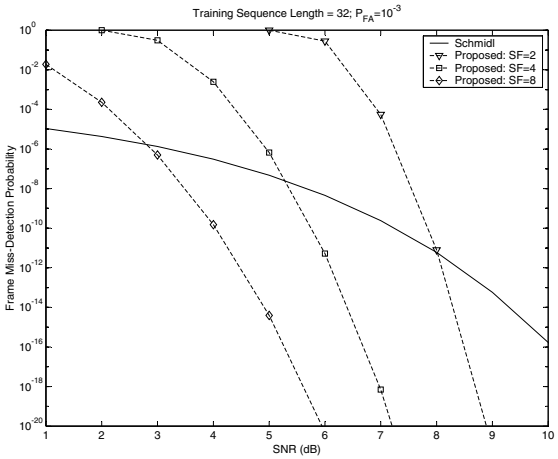

Fig. 2. Frame *Miss Detection* Probability comparison between the proposed scheme and Schmidl method [12] in the multipath channel given by Table.I.

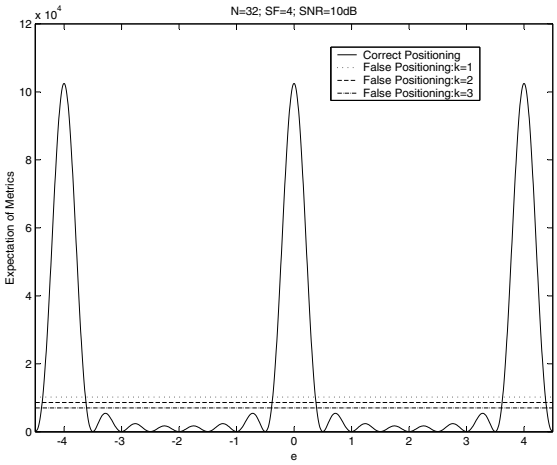

Fig. 3. Expectation of $\Phi_\theta(\hat{\varepsilon})$ and $\Phi_{\theta-k\times SF}(\hat{\varepsilon})$.

TABLE I
MULTIPATH WIRELESS CHANNEL

Carrier	5-GHz			
Bandwidth	10MHz			
DFT Length	256			
Modulation	QPSK			
Carrier Frequency Offset	3.906kHz			
Number of Multipath Taps	4			
Taps Delay (Samples)	0	2	3	6
Channel Attenuation (dB)	0	-3	-6	-9
Initial Phase Distribution	[0,2π)	[0,2π)	[0,2π)	[0,2π)

Miss Detection probability between the proposed method and Schmidl's algorithm. Here we define FRAME *Miss Detection* probability: a new coming frame is assumed to be Miss-Detected if and only if all samples in the training symbol are not detected. Fig. 2 shows that at low SNR, Schmidl's algorithm performs better, and the proposed algorithm outperforms it in high SNR.

IV. JOINT FINE FRAME SYNCHRONIZATION AND CARRIER FREQUENCY OFFSET ACQUISITION

Section III indicates that the proposed Comb-Like training symbol can be detected reliably at the receiver, and achieves coarse timing synchronization. However, power detection can only inform us of the arrival of a new symbol, without indicating the exact start of that symbol. In order to demodulate the transmit signal without introducing ISI, an accurate fine frame synchronization algorithm is needed.

In this section, a new joint fine frame synchronization and carrier frequency offset acquisition is proposed, which is based on a Central-Symmetric and Comb-Like (CSCL) training sequence (the second training symbol of the training sequence is the reverse replica of the first one). Given a normalized carrier frequency offset ε, the relationship between a transmitted sample and its received counterpart is

$$y(n) = v(n-\theta)\cdot e^{\frac{j2\pi\varepsilon n}{N}} + w(n) \quad n \geq 0 \tag{6}$$

where θ indicates the integer-valued timing offset. Joint fine frame synchronization and carrier frequency offset acquisition can be performed as

$$\{\hat{\theta};\hat{\varepsilon}\} = \arg\max_{\{\hat{\theta};\hat{\varepsilon}\}}\{\Phi_{\hat{\theta}}(\hat{\varepsilon})\} \tag{7}$$

where $\Phi_i(\hat{\varepsilon}) = \left|\sum_{n=0}^{N/SF-1}\Psi_i(n)\cdot e^{\frac{j4\pi n\cdot SF\cdot\hat{\varepsilon}}{N}}\right|^2$ with $\Psi_i(n) = y(i+2N-1-n\cdot SF)\cdot y^*(i+n\cdot SF)$ and $n\in[0,N/SF-1]$. When $i=\theta$ (correct timing synchronization is assumed), $\Psi_\theta(n)$ can be represented as $\Psi_\theta(n) = |v(n\times SF)|^2\cdot e^{\frac{j2\pi\varepsilon(2N-1-2n\cdot SF)}{N}} + \eta_n^\theta$, where η_n^θ denotes the noise related items of $\Psi_\theta(n)$. When N/SF is large enough, $\Phi_\theta(\hat{\varepsilon})$ can be approximated as a noncentral chi-square random variable with 2 degrees of freedom [25]. The mean of $\Phi_\theta(\hat{\varepsilon})$ is

$$\mathbb{E}\{\Phi_\theta(\hat{\varepsilon})\} = \sigma_v^4\cdot\frac{\sin^2 2\pi(\hat{\varepsilon}-\varepsilon)}{\sin^2\frac{2\pi(\hat{\varepsilon}-\varepsilon)\cdot SF}{N}} + \sigma_\eta^2, \tag{8}$$

where $\sigma_\eta^2 = \mathbb{E}\{|\eta_n^\theta|^2\}$. $\mathbb{E}\{\Phi_\theta(\hat{\varepsilon})\}$ is a periodic function of $e=\hat{\varepsilon}-\varepsilon$ (carrier frequency offset estimation error) with period $\frac{N}{2\times SF}$. Within each period, since there is one mainlobe, we can uniquely determine ε from $\hat{\varepsilon}$ within one period. Consequently, the maximum carrier frequency offset acquisition range is as large as $\pm\frac{N}{4\times SF}$ times subcarrier spacings. $\mathbb{E}\{\Phi_\theta(\hat{\varepsilon})\}$ will achieve its maximum value if $\hat{\varepsilon}=\varepsilon$.

1-4244-0357-X/06/$20.00 ©2006 Crown Copyright
This full text paper was peer reviewed at the direction of IEEE Communications Society subject matter experts for publication in the IEEE GLOBECOM 2006 proceedings.

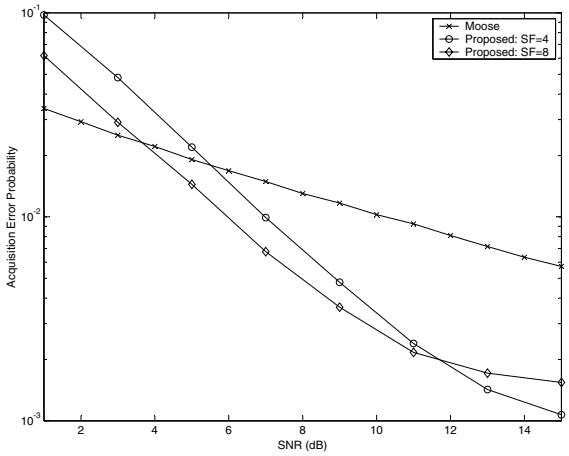

Fig. 4. Performance comparison between the proposed algorithm and the Moose's algorithm with respect to carrier frequency offset acquisition error probability.

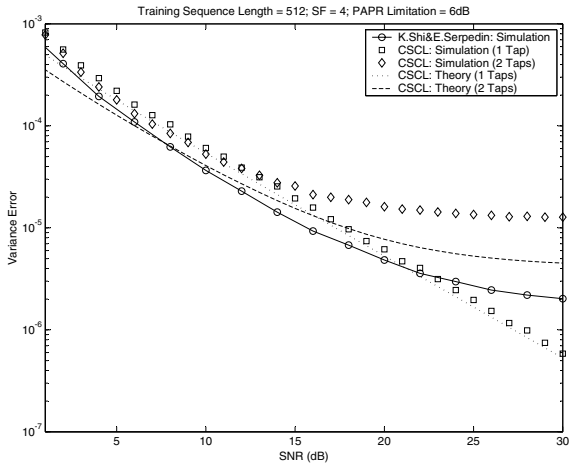

Fig. 5. Performance comparison of the proposed carrier frequency offset fine adjustment algorithm with $SF = 4$ and the K.Shi&E.Serpedin algorithm in the multipath channel.

When $i = \theta - k \times SF$, if N/SF is large enough, $\Phi_{\theta-k\times SF}(\hat{\varepsilon})$ $(0 < k < N/SF)$ can be approximated as a central chi-square random variable with 2 degrees of freedom. The mean and variance of $\Phi_{\theta-k\times SF}(\hat{\varepsilon})$ are $\mathbb{E}\{\Phi_{\theta-k\times SF}(\hat{\varepsilon})\} = \sigma^2$ and $Var\{\Phi_{\theta-k\times SF}(\hat{\varepsilon})\} = \sigma^4$ respectively, with $\sigma^2 = (\frac{N}{SF} - 1 - k)(\sigma_v^4 + 2\sigma_v^2\sigma_w^2 + \sigma_w^4) + (k+1)(\sigma_v^2\sigma_w^2 + \sigma_w^4)$.

$\mathbb{E}\{\Phi_\theta(\hat{\varepsilon})\}$ and $\mathbb{E}\{\Phi_{\theta-k\times SF}(\hat{\varepsilon})\}$ as functions of $e = \hat{\varepsilon} - \varepsilon$ (or $\hat{\varepsilon}$ for a given ε) are illustrated in Fig.3, where we assume that $SNR = 10\,\text{dB}$ and $N = 32$. Within each period, there exists a small vicinity that stands in the center of the main lobe to satisfy $\mathbb{E}\{\Phi_\theta(\hat{\varepsilon})\} > \mathbb{E}\{\Phi_{\theta-k\times SF}(\hat{\varepsilon})\}$. In each main lobe, $\mathbb{E}\{\Phi_\theta(\hat{\varepsilon})\}$ increases as e approaches to the main lobe center. By exploiting this property, a fast joint fine frame synchronization and carrier frequency offset acquisition can be performed.

Correct synchronization can be achieved in the proposed CSCL-based algorithm if and only if timing synchronization and carrier frequency offset acquisition are performed simultaneously. The remaining carrier frequency offset after acquisition should be well within this Fine Adjustment range (i.e., $\left(-\frac{N}{2(2N-1)}, \frac{N}{2(2N-1)}\right)$, which will be discussed in Section V).

Fig. 4 shows a performance comparison between the proposed carrier frequency offset acquisition algorithm and the Moose algorithm, for a wireless system defined in Table I. We also assume that the normalized carrier frequency offset is 1.6 subcarrier bandwidth. In order to perform acquisition correctly, a shortened DFT length of 16 is applied in the Moose's algorithm, with a length-16 CP being padded in front of this shortened training sequence to combat multipath fading. The proposed acquisition scheme outperforms the Moose algorithm when the SNR is larger than 6 dB. Based on its low acquisition error rate, we will assume that the remaining carrier frequency offset after acquisition is well within the Fine Adjustment range of the proposed algorithm.

V. Carrier Frequency Offset Fine Adjustment

After the most of carrier frequency offset being estimated and compensated in Acquisition, the remaining fractional carrier frequency offset can be estimated/corrected with higher accuracy by estimating the phase rotations between correlated blocks in a received training sequence/symbols.

A. Carrier Frequency Offset Fine Adjustment in the AWGN Channels

Define a received CSCL training sequence as $\mathbf{Y}^T = [\mathbf{Y}_1^T\ \mathbf{Y}_2^T]$ where $\mathbf{Y}_1^T = [y(0)\ y(1\times SF)\cdots y(N-SF)]$ and $\mathbf{Y}_2^T = [y(N+SF-1)\ y(2N-1-SF)\cdots y(2N-1)]$. The log-likelihood function $\mathbf{\Lambda}(\varepsilon)$ is the logarithm of the probability density function $f(\mathbf{Y}|\varepsilon)$. Using the correlativity between corresponding samples in $\mathbf{Y}$, $\mathbf{\Lambda}(\varepsilon)$ can be represented as $\mathbf{\Lambda}(\varepsilon) = \log f(\mathbf{Y}|\varepsilon)$. By taking partial derivative to $\mathbf{\Lambda}(\varepsilon)$ with respect to ε and setting the result to zero, we can derive a maximum-likelihood (ML) estimate of ε as

$$\hat{\varepsilon} = \frac{N \sum_{k=0}^{N/SF-1} |\mathbf{\Xi}_k| \cdot (2N-1-2k\cdot SF) \cdot \arg\{\mathbf{\Xi}_k\}}{2\pi \sum_{k=0}^{N/SF-1} |\mathbf{\Xi}_k| \cdot (2N-1-2k\cdot SF)^2} \quad (9)$$

1-4244-0357-X/06/$20.00 ©2006 Crown Copyright
This full text paper was peer reviewed at the direction of IEEE Communications Society subject matter experts for publication in the IEEE GLOBECOM 2006 proceedings.

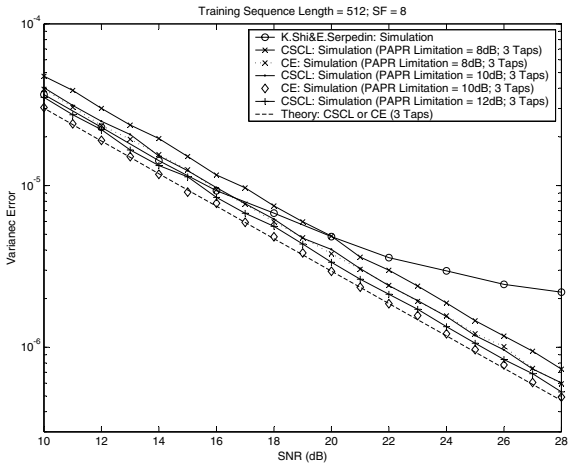

Fig. 6. Performance comparison of the proposed carrier frequency offset fine adjustment algorithm with $SF = 8$ and the K.Shi&E.Serpedin algorithm in the multipath channel.

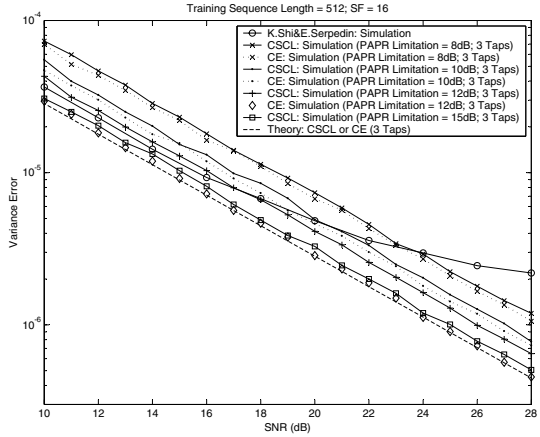

Fig. 7. Performance comparison of the proposed carrier frequency offset fine adjustment algorithm with $SF = 16$ and the K.Shi&E.Serpedin algorithm in the multipath channel.

where $\mathbf{\Xi}_k = y^*(\theta + k \cdot SF) \cdot y(\theta + 2N - 1 - k \cdot SF)$. In order to make Eq.(9) work correctly, $|\arg\{\mathbf{\Xi}_k\}| < \pi$ for each $k \in [0, \frac{N}{SF} - 1]$ should be satisfied ($|\varepsilon| < \frac{N}{2(2N-1)}$). When $SF = 1$, the proposed algorithm reduces to that proposed in [23].

Using the method proposed in [20], the variance error of the proposed algorithm can be derived as

$$Var\{\hat{\varepsilon}\} = \frac{3 \cdot SF \cdot N \cdot [\frac{1}{\mathbf{\Pi}} - (1 + \frac{1}{\mathbf{\Pi}}) \cdot e^{-\mathbf{\Pi}}]}{8\pi^2[2 \cdot SF^2 + (6N - 6) \cdot SF + 4N^2 - 6N + 3]} \tag{10}$$

where $\mathbf{\Pi} = \dfrac{SF^2 \cdot (\bar{\gamma})^2}{2 \cdot SF \cdot \bar{\gamma} + 1}$.

B. Carrier Frequency Offset Fine Adjustment in the Multipath Channels

Note that Eq.(9) was originally derived for AWGN channel, and one expects a performance loss for multipath channels. This performance loss is proportional to the total power of undetected low-power taps. The time-variant baseband multipath channel impulse response is modelled as [25]

$$h(\tau; t) = \sum_{p=1}^{N_p} \rho_p(t) \cdot \delta(\tau - \tau_p(t)) \tag{11}$$

where N_p denotes the number of multipath taps, $\rho_p(t)$ and $\tau_p(t)$ are the complex amplitude and delay of the p-th path, respectively. In this paper, we assume the channel impulse response does not change during one training sequence period, *i.e.*, $\rho_p(t) = \rho_p$ and $\tau_p(t) = \tau_p$. Without loss of generality, we assume $\tau_1 = 0$. Condition of $\sum_{p=1}^{N_p} |\rho_p|^2 = 1$ is assumed here. For the p-th tap, its average SNR is $|\rho_p|^2 \cdot \bar{\gamma}$.

For a given multipath channel, we assume that total m taps each with delay of $D_1, D_2, \cdots, D_m$ samples, respectively, are detected. Based on Eq.(9), the optimized fine adjustment algorithm in the multipath channel can be derived as

$$\hat{\varepsilon} = \frac{\sum_{p=1}^{m} |\rho_p|^2 \cdot \varepsilon_{\hat{D}_p}}{\sum_{p=1}^{m} |\rho_p|^2} \tag{12}$$

where $\varepsilon_{\hat{D}_p} = \frac{N \sum_{k=0}^{N/SF-1} |\mathbf{\Xi}_{k;D_p}| \cdot (2N-1-2k \cdot SF) \cdot \arg\{\mathbf{\Xi}_{k;D_p}\}}{2\pi \cdot \sum_{k=0}^{N/SF-1} |\mathbf{\Xi}_{k;D_p}| \cdot (2N-1-2k \cdot SF)^2}$, $\mathbf{\Xi}_{k;D_p} = y^*(D_p + k \cdot SF) \cdot y(D_p + 2N - 1 - k \cdot SF)$ and $|\rho_p|^2 \cong \frac{\left|\sum_{k=0}^{N/SF-1} \mathbf{\Xi}_{k;D_p}\right|}{\sum_{p=1}^{k} \left|\sum_{k=0}^{N/SF-1} \mathbf{\Xi}_{k;D_p}\right|}$.

VI. PAPR Reduction

The essential advantages of the proposed scheme over conventional algorithms are brought on by the Comb-like shape in the proposed training sequence (CSCL). However, a risk of high PAPR increases simultaneously at these non-zero (power concentrated) samples. In order to reduce the performance loss introduced by PAPR, we alternatively design a time-domain Constant-Envelop (CE) training symbol $\mathbf{v}$ as

$$\begin{aligned} \mathbf{v} = [&\sqrt{\tfrac{SF \cdot P_s}{N}} e^{j\alpha_0}, \underbrace{0, \cdots, 0}_{SF-1}, \sqrt{\tfrac{SF \cdot P_s}{N}} e^{j\alpha_1}, \underbrace{0, \cdots, 0}_{SF-1}, \\ &\cdots, \sqrt{\tfrac{SF \cdot P_s}{N}} e^{j\alpha_{N/SF-1}}, \underbrace{0, \cdots, 0}_{SF-1}]^T \end{aligned} \tag{13}$$

where α_k is a random variable uniformly distributed within $[-\pi, \pi)$.

1-4244-0357-X/06/$20.00 ©2006 Crown Copyright
This full text paper was peer reviewed at the direction of IEEE Communications Society subject matter experts for publication in the IEEE GLOBECOM 2006 proceedings.

VII. Simulation Results

In this paper, a wireless system operating at 5-GHz and with bandwidth of 10 MHz being assumed. A multipath fading environment defined in Table.I is used.

In this section, we performe a comparison between the proposed algorithm (either CSCL-based or CE-based) and the K.Shi&E.Serpedin algorithm [18] with respect to carrier frequency offset estimation accuracy. Simulation results are illustrated in Fig.5 to 7. When $SF = 4$, the performance gain contributed by SF in the proposed algorithm is small, and by utilizing Tap 1, the advantages of the CSCL-based algorithm over the K.Shi&E.Serpedin algorithm becomes significant only at high SNRs. Increasing SF is also an effective route to further improve the performance of the proposed algorithm. For example, even at low SNRs condition, a performance advantage of about 0.3 dB over the K.Shi&E.Serpedin algorithm can be achieved in the CSCL-based algorithm with $SF = 8$ and a PAPR limit of 12 dB. This advantage can be further increased to about 0.5 dB by increasing SF to 16 and adjusting the PAPR limit to 15 dB. As a good tradeoff between high PAPR and high performance gain, the CE-based algorithm improves performance more than the CSCL-based algorithm under the same PAPR limit. For example, in order to provide a performance improvement of about 1 dB over the K.Shi&E.Serpedin algorithm, in the CE-based algorithm at low SNRs condition, we set SF to 8 with a PAPR limit of 10 dB, or to 16 with a PAPR limit of 12 dB.

VIII. Conclusion

In this paper, a new joint frame synchronization and carrier frequency offset estimation scheme has been proposed for burst transmission mode multi-carrier systems. The training sequence has a Comb-like shape with a Central Symmetric structure. The Comb-like shape in the proposed training symbol eases the detection of frames, especially at low SNR. Based on the Central-Symmetric structure of the proposed training sequence, fine frame synchronization as well as carrier frequency offset acquisition can be performed jointly, and the maximum carrier frequency offset acquisition range is up to $\pm\frac{N}{4\times SF}$ times the subcarrier spacing. The comparisons of the proposed algorithm with the K.Shi&E.Serpedin algorithm illustrates the superior performance of the proposed algorithm with regard to estimation accuracy.

References

[1] J. A. C. Bingham, "Multicarrier modulation for data transmission: An idea whose time has come," *IEEE Commun. Mag.*, vol. 28, pp. 5–14, May 1990.

[2] R. van Nee and R. Prasad, *OFDM for Wireless Multimedia Communications*, 1st ed. Artech House, 2000.

[3] B. L. Floch, R. Halbert-Lassalle, and D. Castelain, "Digital sound broadcasting to mobile receivers," *IEEE Trans. Consumer Electron.*, vol. 35, no. 3, pp. 493–503, Aug. 1989.

[4] W. Chen and D. Waring, "Applicability of ADSL to support video dial tone in the copper loop," *IEEE Commun. Mag.*, vol. 32, no. 5, pp. 102–109, May 1994.

[5] IEEE Std 802.11a-1999, "Supplement to IEEE standard for information technology telecommunications and information exchange between systems - local and metropolitan area networks - specific requirements. part 11: wireless lan medium access control (MAC) and physical layer (PHY) specifications: high-speed physical layer in the 5 GHz band," Dec. 1999.

[6] S. Hara and R. Prasad, "Overview of multicarrier CDMA," *IEEE Commun. Mag.*, vol. 35, no. 12, pp. 126–133, Dec. 1997.

[7] H. Atarashi, S. Abeta, and M. Sawahashi, "Variable spreading factor-orthogonal frequency and code division multiplexing (VSF-OFCDM) for broadband packet wireless access," *IEICE Trans. Commun. (Japan)*, vol. E86-B, no. 1, pp. 291–299, Jan. 2003.

[8] W. Warner and C. Leung, "OFDM/FM frame synchronization for mobile radio data communication," *IEEE Trans. Veh. Technol.*, vol. 42, no. 3, pp. 302–313, Aug. 1993.

[9] J. van de Beek, M. Sandell, and P. Borjesson, "ML estimation of time and frequency offset in OFDM systems," *Signal Processing, IEEE Transactions on [see also Acoustics, Speech, and Signal Processing, IEEE Transactions on]*, vol. 45, no. 7, pp. 1800–1805, July 1997.

[10] M.-H. Hsieh and C.-H. Wei, "A low-complexity frame synchronization and frequency offset compensation scheme for OFDM systems over fading channels," *IEEE Trans. Veh. Technol.*, vol. 48, no. 5, pp. 1596–1609, Sept. 1999.

[11] T. Keller, L. Piazzo, P. Mandarini, and L. Hanzo, "Orthogonal frequency division multiplex synchronization techniques for frequency-selective fading channels," *IEEE J. Select. Areas Commun.*, vol. 19, no. 6, pp. 999–1008, June 2001.

[12] T. Schmidl and D. Cox, "Robust frequency and timing synchronization for OFDM," *IEEE Trans. Commun.*, vol. 45, no. 12, pp. 1613–1621, Dec. 1997.

[13] G. Santella, "A frequency and symbol synchronization system for OFDM signals: architecture and simulation results," *IEEE Trans. Veh. Technol.*, vol. 49, no. 1, pp. 254–275, Jan. 2000.

[14] H. Bolcskei, "Blind estimation of symbol timing and carrier frequency offset in wireless OFDM systems," *IEEE Trans. Commun.*, vol. 49, no. 6, pp. 988–999, June 2001.

[15] H. Minn, V. Bhargava, and K. Letaief, "A robust timing and frequency synchronization for OFDM systems," *IEEE Trans. Wireless Commun.*, vol. 2, no. 4, pp. 822–839, July 2003.

[16] S. Barbarossa, M. Pompili, and G. Giannakis, "Channel-independent synchronization of orthogonal frequency division multiple access systems," *IEEE J. Select. Areas Commun.*, vol. 20, no. 2, pp. 474–486, Feb. 2002.

[17] X. Ma, C. Tepedelenlioglu, G. Giannakis, and S. Barbarossa, "Non-data-aided carrier offset estimators for OFDM with null subcarriers: identifiability, algorithms, and performance," *IEEE J. Select. Areas Commun.*, vol. 19, no. 12, pp. 2504–2515, Dec. 2001.

[18] K. Shi and E. Serpedin, "Coarse frame and carrier synchronization of OFDM systems: a new metric and comparison," *IEEE Trans. Wireless Commun.*, vol. 3, no. 4, pp. 1271–1284, July 2004.

[19] P. Moose, "A technique for orthogonal frequency division multiplexing frequency offset correction," *IEEE Trans. Commun.*, vol. 42, no. 10, pp. 2908–2914, Oct. 1994.

[20] Z. Zhang, W. Jiang, H. Zhou, Y. Liu, and J. Gao, "High accuracy frequency offset correction with adjustable acquisition range in OFDM systems," *IEEE Trans. Wireless Commun.*, vol. 4, no. 1, pp. 228–237, Jan. 2005.

[21] M. Luise and R. Reggiannini, "Carrier frequency acquisition and tracking for OFDM systems," *IEEE Trans. Commun.*, vol. 44, no. 11, pp. 1590–1598, Nov. 1996.

[22] M. Morelli and U. Mengali, "An improved frequency offset estimator for OFDM applications," *IEEE Commun. Lett.*, vol. 3, no. 3, pp. 75–77, Mar. 1999.

[23] Z. Zhang, M. Zhao, H. Zhou, Y. Liu, and J. Gao, "Frequency offset estimation with fast acquisition in OFDM system," *IEEE Commun. Lett.*, vol. 8, no. 3, pp. 171–173, Mar. 2004.

[24] H. Liu and U. Tureli, "A high-efficiency carrier estimator for OFDM communications," *IEEE Commun. Lett.*, vol. 2, no. 4, pp. 104–106, Apr. 1998.

[25] J. G. Proakis, *Digital Communications*, 4th ed. McGraw-Hill, 2001.

[26] D. Rife and R. Boorstyn, "Single tone parameter estimation from discrete-time observations," *IEEE Trans. Inform. Theory*, vol. 20, pp. 591–598, Sept. 1974.

1-4244-0357-X/06/$20.00 ©2006 Crown Copyright

This full text paper was peer reviewed at the direction of IEEE Communications Society subject matter experts for publication in the IEEE GLOBECOM 2006 proceedings.